

Adsorption of reactive dye onto cross-linked chitosan/oil palm ash composite beads

M. Hasan, A.L. Ahmad, B.H. Hameed*

*School of Chemical Engineering, Engineering Campus, University Science Malaysia,
14300 Nibong Tebal, Penang, Malaysia*

Received 13 December 2006; received in revised form 14 February 2007; accepted 21 March 2007

Abstract

Adsorption of reactive dye from aqueous solution onto cross-linked chitosan/oil palm ash composite beads (CC/OPA) was investigated in a batch system. Kinetic and isotherm studies were carried out by considering the effects of various parameters, such as initial concentration (50–500 mg/L), contact time, pH (2–13), and temperature (30, 40, 50 °C). It was found that the dye uptakes were much higher in acidic solutions than those in neutral and alkaline conditions. Langmuir, Freundlich, Redlich–Peterson, and Temkin isotherms were used to analyze the equilibrium data at different temperatures. The Redlich–Peterson isotherm fits the experimental data significantly better than the other isotherms. Adsorption kinetics data were tested using pseudo-first-order and pseudo-second-order models. Kinetic studies showed that the adsorption followed a pseudo-second-order model. The pseudo-first-order and pseudo-second-order rate constants for different initial concentrations were evaluated and discussed. Thermodynamic parameters such as standard Gibbs free energy (ΔG°), standard enthalpy (ΔH°), and standard entropy (ΔS°) were evaluated by applying the Van't Hoff equation. The thermodynamics of reactive dye adsorption onto cross-linked chitosan/oil palm ash composite beads indicates its spontaneous and endothermic nature.

© 2007 Elsevier B.V. All rights reserved.

Keywords: Adsorption; Cross-linked chitosan/oil palm ash composite beads; Reactive blue 19; Isotherms; Kinetics

1. Introduction

The major problems concerning environmental pollutants is removing colour from water and wastewater industrial activities. Dyes are released into wastewaters from various industrial units, mainly from the dye manufacturing and textiles and other fabric finishing [1]. Most dyes are non-biodegradable in nature, which are stable to light and oxidation. Therefore, the degradation of dyes in wastewater either traditional chemical or biological process has not been very effective [2–4].

Reactive dyes are most problematic compounds among other dyes in textile wastewater. Reactive dyes are highly water-soluble and estimated that 10–20% of reactive dyes remain in the wastewater during the production process of these dyes [5] and nearly 50% of reactive dyes may be lost to the effluent during dyeing processes of cellulose fibers [6]. Reactive dye wastewater has limited biodegradability in an aerobic environment and many azo dyes under anaerobic conditions decompose into potentially carcinogenic aromatic amines [7,8].

Adsorption process has been found becoming a prominent method of treating aqueous effluent in industrial processes for a variety of separation and purification purpose [9]. This technique also found to be highly efficient for the removal of colour in terms of initial cost, simplicity of design, ease of operation and insensitivity to toxic substances [10]. Therefore, adsorption using activated carbon is currently of great interest for removal of dyes and pigments. In spite of its prolific use, activated carbon remains an expensive material since higher the quality of activated carbon, the greater in cost. This has led to the search for cheaper substitutes. Today, attention has been focused on the low-cost adsorbents as alternative adsorbent materials such as oil palm ash [11]. This ash is produced after combustion of oil palm fiber and shell as boiler fuel to produce steam for palm-oil mill consumption. This solid waste is highly abundant in Malaysia, which is one of the largest palm-oil exporters in the world. Malaysia thus generates huge loads of palm ash each year. The oil palm ash showed very high adsorption capacity to remove direct dye [11].

Recently, chitosan that is used as an adsorbent has drawn attentions due to its high contents of amino and hydroxy functional groups showing high potentials of the adsorption

* Corresponding author. Tel.: +60 4 599 6422; fax: +60 4 594 1013.
E-mail address: chbassim@eng.usm.my (B.H. Hameed).

Nomenclature

a_R	constant of Redlich–Peterson (L/mg)
A	Arrhenius factor
b	Langmuir constant (L/mg)
B_1	Temkin isotherm constant
C_e	equilibrium liquid-phase solute concentration (mg/L)
C_0	initial liquid-phase solute concentration (mg/L)
E	mean energy of adsorption (kJ/mol)
E_a	Arrhenius activation energy of sorption (kJ/mol)
ΔG°	Gibbs free energy of adsorption (kJ/mol)
ΔH°	enthalpy of adsorption (kJ/mol)
k_a	adsorption rate constant
k_d	desorption rate constant
k_1	pseudo-first-order rate constant (1/h)
k_2	pseudo-second-order rate constant (g/mg h)
K_C	equilibrium constant
K_F	Freundlich constant ((mg/g) (L/mg) ^{1/n})
K_R	Redlich–Peterson isotherm constant (L/g)
K_t	equilibrium binding constant (L/mg)
n	Freundlich isotherm constant related to adsorption intensity
q_e	amount of adsorption at equilibrium (mg/g)
$q_{e\text{ cal}}$	calculated value of adsorbate concentration at equilibrium (mg/g)
$q_{e\text{ exp}}$	experimental value of adsorbate concentration at equilibrium (mg/g)
q_m	maximum adsorption capacity of adsorbent per unit mass (mg/g)
q_t	amount of adsorbate adsorbed by adsorbent at time t (mg/g)
Q_0	Langmuir constant (mg/g)
R	universal gas constant (8.314 J/mol K)
R_L	dimensionless constant separation factor
R^2	correlation coefficient
ΔS°	entropy of adsorption
t	time (h)
T	absolute temperature (K)
V	volume of the solution (L)
W	mass of dry adsorbent (g)
<i>Greek letter</i>	
β	constant of Redlich–Peterson isotherm

of dyes [12], metal ions [13] and proteins [14]. Chitosan is the deacetylated form of chitin, which is linear polymer of acetylamino-D-glucose. Other useful features of chitosan include its abundance, non-toxicity, hydro-philicity, biocompatibility, biodegradability and anti-bacterial property [15]. Moreover, the adsorption of reactive dyes, basic dyes and acidic dyes in natural solutions using chitosan shows large adsorption capacities [12,16].

Many textile wastewaters are highly acid. In acid aqueous solutions, the amino groups of chitosan are much easier to be

cationized and they adsorb the dye anions strongly by electrostatic attraction [15]. However, chitosan formed gels below pH 5.5 and could not be evaluated. This problem limits the use of chitosan as adsorbent for dye removal, as this compound is highly soluble in such environments. This has led to prepare cross-linked chitosan adsorbent which is necessary to stabilize the prepared adsorbent in acid medium as well as to grant the material the mechanical strength necessary for the adsorption studies in dynamic systems. Yoshida et al. [17] used Denacol EX841 as a cross-linking reagent and obtained a high adsorption capacity (1200–1700 g/kg) of orange II (AO7) on the cross-linked chitosan fibers in acid solutions of pH 3.0 and 4.0. Chiou and Li [18] prepared cross-linked chitosan by epichlorohydrin (ECH) and exhibited a high adsorption capacity (1802–1840 g/kg) of reactive dye (RR189) on the cross-linked chitosan beads in acid aqueous solutions at 30 °C and pH 3.0.

The aim of this study was to investigate the adsorption of reactive blue 19 (RB19) dye onto cross-linked chitosan/oil palm ash composite beads, which is a low-cost adsorbent for the removal of dye.

2. Materials and methods

2.1. Adsorbate: reactive blue 19

The reactive blue 19 (RB19) used in this work was obtained from Sigma–Aldrich, Malaysia and used without further purification. The dye was chosen as adsorbate because it is very important in dyeing of cellulosic fibers and is regarded as dye contaminant in the discharged effluent. The properties of RB19 are summarized in Table 1. The aqueous solution was prepared by dissolving solute in deionized water to the required concentrations without any pH adjustment. The wavelength of maximum absorbance (λ_{max}) for RB19 was 598 nm.

2.2. Chitosan and oil palm ash

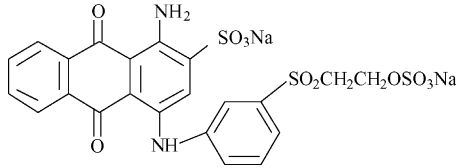
The chitosan derived from deacetylated lobster shell wastes was supplied by Hunza Pharmaceutical Sdn Bhd., Nibong Tebal, Malaysia. The chitosan was washed three times with deionized water and dried in an oven at 50 °C before use. Some properties of chitosan are given in Table 2.

The oil palm ash (OPA) was provided by United Oil Palm Mill, Penang, Malaysia. It was sieved through a stack of U.S. standard sieves and the fine particle size of 63 μm was used. Then, OPA was washed with deionized water and oven dried overnight at 110 °C. OPA (50 g) was activated by refluxing with 250 mL of 1 mol/L H_2SO_4 at 80 °C in a round-bottom flask for 4 h. The slurry was air-cooled and filtered with a glass fiber. The filter cake was repeatedly washed with deionized water until the filtrate was neutral. It was then dried in an oven at 110 °C before use.

2.3. Preparation of chitosan/oil palm ash composite beads

Chitosan (1 g) was dissolved in 1 mol/L acetic acid (100 mL) and mixed with activated oil palm ash (1 g) and agitated for

Table 1
Properties of reactive blue 19

Chemical index (CI)	No. 61200
Class	Anthraquinone
Ionisation	Acid
Maximum wavelength, λ_{\max} (nm)	598
Colour	Blue
Relative molecular weight	626.56
Chemical structure	

1 h. Then, the viscous solution was sprayed dropwise through a syringe, at a constant rate, into neutralization solution containing 15% NaOH and 95% ethanol in a volume ratio of 4:1. They were left in the solution for 1 day [19]. The formed composite beads were washed with deionized water until solution become neutral and then stored in distilled water.

2.4. Preparation of cross-linked chitosan/oil palm ash composite beads

Epichlorohydrin (ECH) purchased from Sigma–Aldrich was used as cross-linking agent in this study. The procedure for cross-linking was same as reported previously [18]. Basically, wet non-cross-linked chitosan/oil palm ash composite beads (0.1 g dry basis of chitosan) and 50 cm³ of 1N sodium hydroxide solution were poured together in a 500 cm³ flask. ECH was added into the above solution, and shaken for 6 h at 50 °C with water bath. The molar ratio of cross-linking reagent/chitosan was 0.5. The cross-linking chitosan/oil palm ash composite beads (CC/OPA) were filtered out, washed with deionized water and stored in distilled water. Then, the beads (2–3 mm) were dried in a freeze dryer for 6 h before used as adsorbent.

2.5. Batch equilibrium studies

Adsorption isotherms were performed in a set of 43 Erlenmeyer flasks (250 mL), where solutions of dye (100 mL) with different initial concentrations (50–500 mg/L) were placed in these flasks. The original pH (6) of the solutions was used. Equal masses of 0.2 g of particle size (2–3 mm) CC/OPA (adsorbent) were added to dye solutions, and the mixtures were then kept in an isothermal shaker (30 ± 0.1 °C) for 48 h to reach equilibrium. A similar procedure was followed for another set of

Erlenmeyer flask containing the same dye concentration without adsorbent to be used as a blank. The flasks were then removed from the shaker, and the final concentration of dye in the solution was measured at 598 nm, using UV–vis spectrophotometer (Shimadzu UV/Vis 1601 spectrophotometer, Japan). The amount of adsorption at equilibrium time t , q_e (mg/g), is calculated by

$$q_e = \frac{(C_0 - C_e)V}{W} \quad (1)$$

where C_0 and C_t (mg/L) are the liquid-phase concentrations of dye at initial and any time t , respectively; V the volume of the solution (L); W is the mass of dry adsorbent used (g).

To study the effect of initial pH on the RB19 removal by CC/OPA, the pH was adjusted by adding a few drops of dilute 1.0 M NaOH or 1.0 M HCl before each experiment. Experimental conditions consisted of 0.2 g adsorbent, 100 mL of 200 mg/L RB19 solution, temperature equal to 30 °C and contact time 48 h. The effect of temperature (at 30, 40 and 50 °C) on the adsorption of RB19 by CC/OPA was studied at pH 6.0, 0.2 g adsorbent and initial RB19 concentration of 50–500 mg/L for 48 h.

2.6. Batch kinetic studies

The procedures of kinetic experiments are basically identical to those of equilibrium tests. The aqueous samples were taken at present time intervals, and the concentrations of dye were similarly measured.

The amount of adsorption at time t , q_t (mg/g), is calculated by

$$q_t = \frac{(C_0 - C_t)V}{W} \quad (2)$$

where C_0 and C_t (mg/L) are the liquid-phase concentrations of dye at initial and any time t , respectively; V the volume of the solution (L); W is the mass of dry adsorbent used (g).

3. Results and discussion

3.1. Effect of solution pH

Fig. 1 shows the effect of pH on adsorption of RB19 onto CC/OPA at 30 °C and initial dye concentration 200 mg/L, particle size 2–3 mm. The adsorption of RB19 was studied over

Table 2
Properties of chitosan flake^a

Deacetylation degree	>90.0%
Solubility in 1% acetic acid	>99.0%
Moisture	<10.0%
Ash content	<1.0%
Appearance	Off-white

^a Hunza Pharmaceutical Sdn. Bhd.

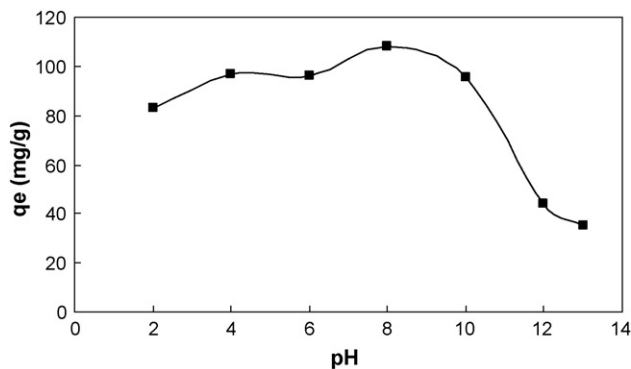


Fig. 1. Effect of pH on the RB19 adsorption ($C_0 = 200$ mg/L, $T = 30$ °C).

a pH range 2–13 and the studies were carried out for 48 h. Fig. 1 indicates that the pH is significantly affected the adsorption of the reactive blue 19 onto CC/OPA. It was clear that the dye uptakes were much higher in acidic solutions than those in neutral and alkaline conditions. Yoshida et al. [16] and Kumar [15] reported that at lower pH more protons will be available to protonate amino groups of chitosan molecules to form groups $-\text{NH}_3^+$, thereby increasing the electrostatic attractions between negatively charged dye anions and positively charged adsorption sites and causing an increase in dye adsorption. This explanation agrees well with our result on pH effect. Similar result was also reported for the adsorption of RR 189 (reactive dye) on cross-linked chitosan beads [18]. From pH 10.0 to 13.0, the adsorption was lower than at acidic solution. This might be explained by the fact that chemical cross-linking reduces either the total number and/or the diameter of the pores in chitosan beads, making the dye molecule more difficult to transfer [18].

3.2. Effect of initial dye concentration

The adsorption of dye by CC/OPA was studied at different initial RB19 concentrations ranging from 50 to 500 mg/L. Fig. 2 shows the result for effect of initial dye concentration on adsorption of RB19 onto CC/OPA at pH 6. As can be seen from Fig. 2, the amount of the adsorbed dye at low initial concentration (50–200 mg/L) achieve adsorption equilibrium in about 4 h, at some point in time, reaches a constant value beyond which

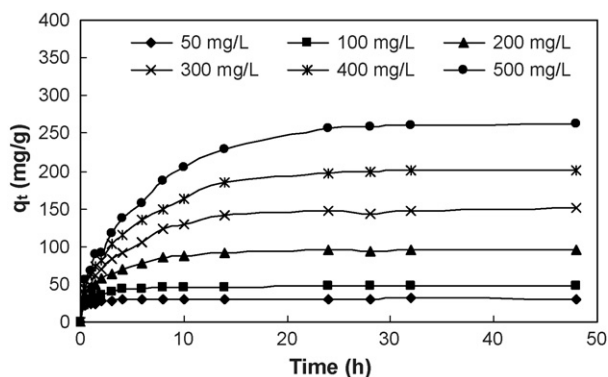


Fig. 2. Effect of initial concentration on the adsorption of RB19 on CC/OPA at pH 6, 30 °C.

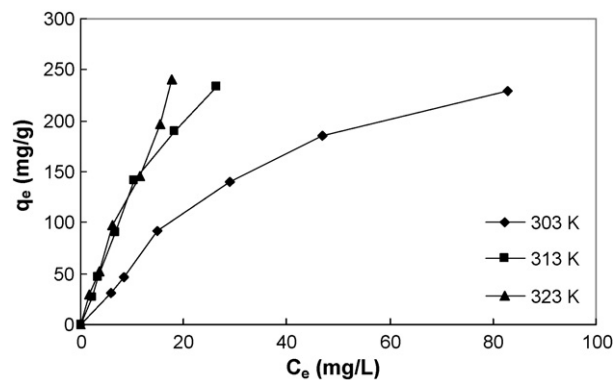


Fig. 3. Effect of temperature on the adsorption of RB19 on CC/OPA.

no more is removed from solution. While at high initial dye concentration (300–500 mg/L), the time necessary to reach equilibrium was about 24 h. However, the experimental data were measured at 48 h to make sure that full equilibrium was attained. The adsorption capacity at equilibrium increases from 43.4 to 423.5 mg/g, with increase in the initial dye concentration from 50 to 500 mg/L. An increase in initial dye concentration leads to increase in the adsorption capacity of dye on CC/OPA. This indicates that initial dye concentrations played an important role in the adsorption of RB19 on the CC/OPA. A similar phenomenon was observed for the adsorption of reactive blue 15 dye from an aqueous solution on cross-linked chitosan beads [20] and drim yellow-K4G on the shale oil ash [21].

3.3. Effect of temperature

A study of the temperature dependence of adsorption process gives valuable information about the enthalpy during adsorption. The effect of temperature on the adsorption isotherm was studied by carrying out a series of isotherms at 30, 40 and 50 °C as shown in Fig. 3. At temperature 50 °C, more dye strongly adsorbed by the CC/OPA and thus induced a higher Q_0 value (Table 3). This process was endothermic, where increasing the temperature increases the value of Q_0 .

3.4. Adsorption isotherm

The adsorption isotherm is the most important information which indicates how the adsorbate molecules distribute between the liquid phase and the solid phase when the adsorption process reaches an equilibrium state. To optimize the design of an adsorption system for the adsorption of adsorbates, it is important to establish the most appropriate correlation for the equilibrium curves. Various isotherm equations like those Langmuir, Freundlich, Redlich–Peterson, Tempkin and Dubinin–Ruduskevich were used to describe the equilibrium characteristics of adsorption.

The linear form of Langmuir isotherm is expressed as

$$\frac{C_e}{q_e} = \frac{1}{Q_0 b} + \frac{C_e}{Q_0} \quad (3)$$

Table 3
Langmuir, Freundlich, Redlich–Peterson and Temkin isotherm model constants and correlation coefficients for adsorption of RB19 onto CC/OPA

Temperature (°C)	b (L/mg)	Q_0 (mg/g)	R_L	R^2
Langmuir isotherm				
30	0.016	416.7	0.111	0.93
40	0.022	666.7	0.133	0.72
50	0.018	909.1	0.154	0.60
Temperature (°C)	K_F	n	R^2	
Freundlich isotherm				
30	9.619	1.318	0.96	
40	15.427	1.147	0.97	
50	18.302	1.144	0.99	
Temperature (°C)	K_R	a_R	β	R^2
Redlich–Peterson isotherm				
30	7.626	0.021	0.9991	1.00
40	17.360	0.040	0.9649	0.99
50	22.310	0.414	0.1879	0.99
Temperature (°C)	K_T (L/mg)	B_1	R^2	
Temkin isotherm				
30	0.232	76.617	1.00	
40	0.519	85.098	0.98	
50	0.630	85.370	0.91	

where q_e is the amount of dye adsorbed per unit weight of adsorbent (mg/g) and C_e is the equilibrium concentration of dye in solution (mg/L). The constant Q_0 signifies the adsorption capacity (mg/g) and b is related with the energy of the adsorption (L/mg). A plot of C_e/q_e versus C_e (Fig. 4) yields a straight line with slope $1/Q_0$ and intercept $1/Q_0b$. Table 3 lists that the computed maximum adsorption capacity Q_0 of RB19 onto the CC/OPA at different temperatures.

The essential characteristics of the Langmuir isotherm can be expressed in terms of dimensionless constant separation factor R_L given by [22]:

$$R_L = \frac{1}{1 + bC_0} \quad (4)$$

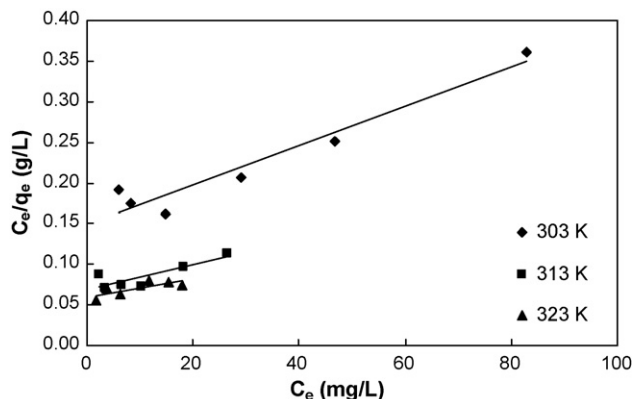


Fig. 4. Linearized Langmuir isotherms at different temperatures.

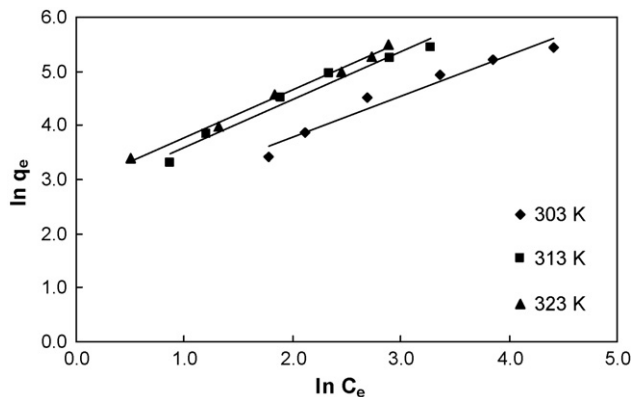


Fig. 5. Linearized Freundlich isotherms at different temperatures.

where b is the Langmuir constant and C_0 is the highest initial dye concentration (mg/L). According to the value of R_L the isotherm shape may be interpreted as follows:

Value of R_L	Type of adsorption
$R_L > 1.0$	Unfavourable
$R_L = 1.0$	Linear
$0 < R_L < 1.0$	Favourable
$R_L = 0$	Irreversible

Values of R_L calculated at 30, 40 and 50°C were in range between 0 and 1 which indicate that the adsorption is favourable at operation conditions studied.

The Freundlich isotherm [23] is an empirical equation based on a heterogeneous surface. A linear form of the Freundlich expression will yield the constants K_F and n . Hence

$$\ln q_e = \ln K_F + \frac{1}{n} \ln C_e \quad (5)$$

therefore, a plot of $\ln q_e$ versus $\ln C_e$ (Fig. 5) enables the constant K_F and exponent n to be determined. K_F can be defined as adsorption of distribution coefficient and represents the quantity of dye adsorbed onto adsorbent for an equilibrium concentration. The slope $1/n$, ranging between 0 and 1, is a measure of adsorption intensity or surface heterogeneity, becoming more heterogeneous as its value gets closer to zero. These values together with the correlation coefficient are presented in Table 3.

Based on the correlation coefficient (R^2) shown in Table 3, the adsorption isotherm with CC/OPA can be described by Freundlich equation. Also, the Freundlich equation yields a better fit of the experimental data than Langmuir equation (Fig. 5). In principle, the Freundlich equation is an empirical approach for adsorbent with very uneven adsorbing surface, and is applicable to the adsorption of single solutes within a fixed range of concentration.

Another equation used in the analysis of isotherms was proposed by Temkin and Pyzhev [24]. Temkin isotherm contains a factor that explicitly takes into account adsorbing species–adsorbate interactions. This isotherm assumes that: (i) the heat of adsorption of all the molecules in the layer decreases linearly with coverage due to adsorbate–adsorbate interactions,

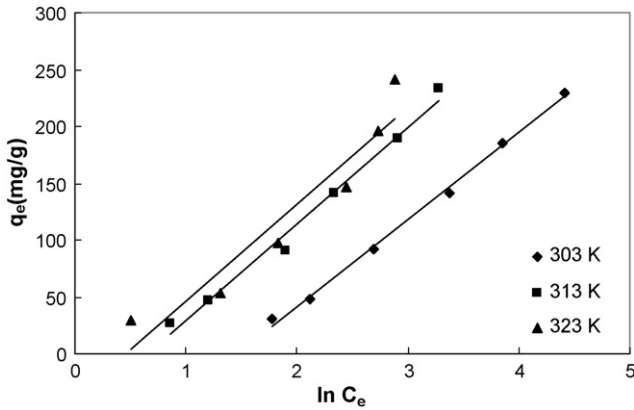


Fig. 6. Temkin isotherms at different temperatures.

and (ii) adsorption is characterized by a uniform distribution of binding energies, up to some maximum binding energy [24,25]. Temkin isotherm is represented by the following equation:

$$q_e = \frac{RT}{b} \ln(K_t C_e) \tag{6}$$

Eq. (6) can be expressed in its linear form as

$$q_e = B_1 \ln K_t + B_1 \ln C_e \tag{7}$$

where

$$B_1 = \frac{RT}{b} \tag{8}$$

the adsorption data can be analyzed according to Eq. (7). A plot of q_e versus $\ln C_e$ enables the determination of the isotherm constants K_t and B_1 . K_t is the equilibrium binding constant (L/mg) corresponding to the maximum binding energy and constant B_1 is related to the heat of adsorption. This isotherm is plotted in Fig. 6 and values of the parameters are given in Table 3.

Redlich and Peterson [26] incorporate three parameters into an empirical isotherm. The Redlich–Peterson isotherm has a linear dependence on concentration in the numerator and an exponential function in the denominator. It approaches the Freundlich model at high concentration and is in accordance with the low concentration limit of the Langmuir equation. Furthermore, the R–P equation incorporates three parameters into an empirical isotherm, and therefore, can be applied either in homogeneous or heterogeneous systems due to the high versatility of the equation. It can be described as follows:

$$q_e = \frac{K_R C_e}{1 + a_R C_e^\beta} \tag{9}$$

where K_R is the R–P isotherm constant (L/g); a_R the R–P isotherm constant (L/mg); β is the exponent which lies between 1 and 0, where $\beta = 1$:

$$q_e = \frac{K_R C_e}{1 + a_R C_e} \tag{10}$$

It becomes a Langmuir equation. Where $\beta = 0$:

$$q_e = \frac{K_R C_e}{1 + a_R} \tag{11}$$

i.e. the Henry’s law equation.

Eq. (9) can be converted to a linear form by taking logarithms:

$$\ln \left(K_R \frac{C_e}{q_e} - 1 \right) = \ln a_R + \beta \ln C_e \tag{12}$$

The constants were determined by non-linear regression using MATLAB. The R–P isotherm constants a_R , K_R and β and the correlation coefficients, R^2 , for the R–P isotherm are shown in Table 3. The correlation coefficients are significantly higher than the Langmuir isotherm R^2 values. Based on the values of correlation coefficients listed in Table 3, we can conclude that the Redlich–Peterson isotherm fits the experimental data for RB19 adsorption significantly better than the other isotherms.

3.5. Adsorption kinetics

In order to investigate the mechanism of adsorption, the pseudo-first-order and pseudo-second-order equations were used to test the experimental data of initial concentration. The Lagergren [27] rate equation, which is the first rate equation developed for sorption in liquid/solid systems, is based on solid capacity. The pseudo-first-order equation is represented as

$$\log(q_e - q_t) = \log q_e - \frac{k_1}{2.303} t \tag{13}$$

where q_e and q_t are the amounts of dye adsorbed on adsorbent at equilibrium and at time t , respectively (mg/g). The slope and intercept of plot of $\log(q_e - q_t)$ versus t were used to determine the pseudo-first-order rate constant k_1 (h^{-1}) (Fig. 7).

The pseudo-second-order kinetic model [28,29] expressed as

$$\frac{t}{q_t} = \frac{1}{k_2 q_e^2} + \frac{t}{q_e} \tag{14}$$

where k_2 (g/mg h) is the rate constant of pseudo-second-order adsorption. If pseudo-second-order kinetics is applicable, the plot t/q_t versus t shows a linear relationship. There is no need to know any parameter beforehand and q_e and k_2 can be determined from the slope and intercept of the plot (Fig. 8). Also, it is more likely to predict the behavior over the whole the range

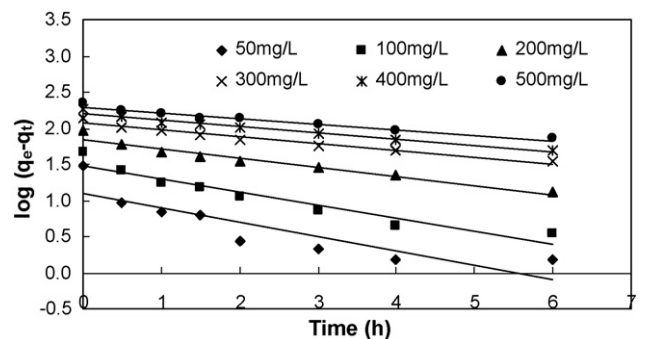


Fig. 7. Pseudo-first-order kinetics of RB19 adsorption onto CC/OPA at various initial concentrations (pH 6.0 at 30 °C).

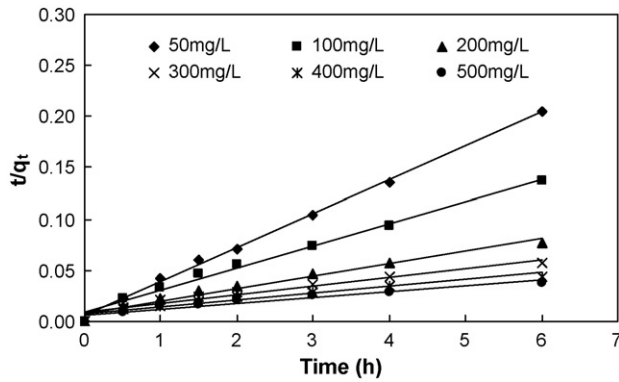


Fig. 8. Pseudo-second-order kinetics of RB19 adsorption onto CC/OPA at various initial concentrations (pH 6.0 at 30 °C).

of adsorption and is in agreement with chemical sorption being the rate-controlling step [30] which may involve valency forces through sharing or exchange of electrons between dye anions and adsorbent.

The correlation coefficients of the pseudo-second-kinetic model for the linear plots are more than 0.92. The values of the parameters k_1 , k_2 were also calculated and summarized in Table 4. Based on the results of correlation coefficients, at initial concentrations 50–200 mg/L, the adsorption kinetics obeys a pseudo-second-order model, while at higher concentrations (300–500 mg/L) it obeys a pseudo-first-order model. This result means that sometimes the correlation coefficient is not a sufficient criteria for selection of an adsorption kinetic model [31]. Aziaian [32] derived theoretically that the pseudo-first-order rate coefficient (k_1) is not the intrinsic adsorption rate constant but is a combination of adsorption (k_a) and desorption (k_d) rate constants [32] as

$$k_1 = k_a C_0 + k_d \quad (15)$$

According to Eq. (15), if the adsorption kinetic follows pseudo-first-order, then its rate coefficient is a linear form. Table 4 shows that the relation between k_1 versus C_0 is not linear and also decrease with increasing C_0 (figure not shown). Therefore, it is concluded that in the initial concentration between 300 and 500 mg/L the adsorption of RB19 on CC/OA does not obey the pseudo-first-order model.

Azizian [32] also reported that the rate coefficient of pseudo-second-order rate model (k_2) is a complex function of the initial concentration of solute (C_0). Inspection the results shown in Table 4, when the rate coefficient of the pseudo-second-order

Table 5

Thermodynamic parameters for the adsorption of RB19 on CC/OPA

E_a (kJ/mol)	12.9
ΔH° (kJ/mol)	46.2
ΔS° (J/mol K)	166.2
ΔG° (kJ/mol)	
303 K	−3.86
313 K	−6.43
323 K	−7.15

rates model (k_2) was plotted versus initial concentration of RB19 (figure not shown), the relation between k_2 and C_0 is not a simple function. Therefore, the adsorption of RB19 onto CC/OPA followed a pseudo-second-order model. This result agreed with that of adsorption of 18-crown-6 from aqueous solution on a granular activated carbon [31].

3.6. Adsorption thermodynamic

In order to evaluate the thermodynamic parameters for adsorption of RB19 on CC/OPA, the adsorption studies were carried out at different temperatures 30, 40 and 50 °C. The adsorption standard free energy changes (ΔG°) can be calculated according to:

$$\Delta G^\circ = -RT \ln K_C \quad (16)$$

$$K_C = \frac{q_e}{C_e} \quad (17)$$

where R is the universal gas constant (8.314 J/mol K); q_e the amount of dye (mg) adsorbed on the adsorbent per liter of the solution at equilibrium; C_e the equilibrium concentration (mg/L) of the dye in the solution; T is the temperature in K. The average standard enthalpy change (ΔH°) is obtained from Van't Hoff equation:

$$\ln K_C = \frac{\Delta S^\circ}{R} + \frac{\Delta H^\circ}{RT} \quad (18)$$

where K_C is the equilibrium constant; T the solution temperature (K); R is the gas constant. ΔH° and ΔS° were calculated from the slope and intercept of plot of $\ln K_C$ versus $1/T$. The results are given in Table 5.

The results show that the enthalpy of adsorption ΔH° for RB19 was 46.2 kJ/mol. A positive standard enthalpy change (ΔH°) suggests that the interaction of RB19 adsorbed by

Table 4
Kinetic parameters of RB19 adsorbed onto CC/OPA at different initial concentrations

C_0 (mg/L)	$q_{e \text{ exp}}$ (mg/g)	Pseudo-first-order kinetic model			Pseudo-second-order kinetic model		
		$q_{e \text{ cal}}$ (mg/g)	k_1 (h^{-1})	R^2	$q_{e \text{ cal}}$ (mg/g)	k_2 (g/mg h)	R^2
50	30.81	12.49	0.46	0.76	30.12	0.19	1.00
100	47.40	30.54	0.42	0.91	46.51	0.05	0.99
200	91.53	69.57	0.29	0.95	82.64	0.02	0.97
300	140.71	117.54	0.22	0.96	116.28	0.01	0.95
400	185.73	159.85	0.20	0.97	149.25	0.01	0.93
500	229.28	197.83	0.18	0.96	175.44	0.01	0.92

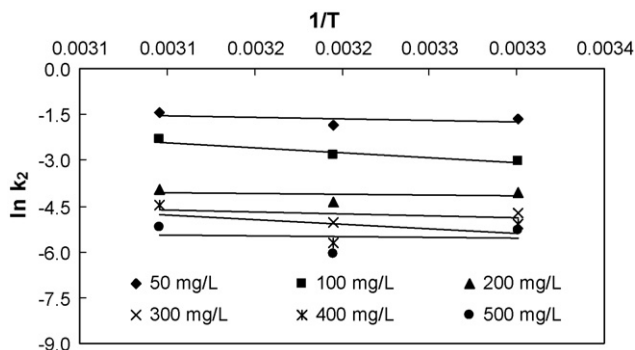


Fig. 9. Plots of $\ln(k_2)$ against reciprocal temperature for RB19 adsorption onto CC/OPA.

CC/OPA is endothermic, which is supported by the increasing adsorption of RB19 with the increase in temperature while a negative adsorption standard free energy change (ΔG°) and a positive standard entropy change (ΔS°) indicate that the adsorption reaction is a spontaneous process [33] and more favorable at high temperature. Generally, the absolute magnitude of the change in free energy for physical adsorption is smaller than that of chemisorption. The former ranges from -20 to 0 kJ/mol, and the latter ranges from -80 to -400 kJ/mol [34]. When the temperature increased from 30 to 50 °C, ΔG° was increased from -3.86 to -7.15 kJ/mol. This could be considered as physical adsorption and more favorable at high temperature.

The pseudo-second-order rate constant of dye adsorption is expressed as a function of temperature by the Arrhenius type relationship:

$$\ln k_2 = \ln A - \frac{E_a}{RT} \quad (19)$$

where E_a is the Arrhenius activation energy of sorption, representing the minimum energy that reactants must have for the reaction to proceed; A the Arrhenius factor; R the gas constant; T is the solution temperature. When $\ln k_2$ is plotted versus $1/T$ (Fig. 9), a straight line with slope $-E_a/R$ is obtained. The chemisorption or physisorption mechanisms are often an important indicator to describe the type of interaction between dye molecule and adsorbent. The physisorption processes usually have energies in the range of 4 – 40 kJ/mol, while higher activation energies (40 – 400 kJ/mol) suggest chemisorption [35]. The value of E_a was 12.9 kJ/mol and indicates that process was physisorption mechanism.

4. Conclusions

This study confirmed that cross-linked chitosan/oil palm ash composite beads were an excellent adsorbent for removal of reactive blue 19 dye from aqueous solution. The maximum adsorption observed at pH 6 for cross-linked chitosan/oil palm ash composite beads. A decrease in the pH of solutions leads to a significant increase in the adsorption capacity of dye RB19 on the adsorbent. Langmuir, Freundlich, Redlich–Peterson, and Temkin isotherm equation were used to describe the adsorp-

tion of RB19 onto CC/OPA. Redlich–Peterson showed better correlation coefficient than the other models at all temperatures studied. The prepared adsorbent exhibits a high adsorption capacity to remove RB19, whose adsorption maximum monolayer adsorption capacity is greater than 400 mg/g at pH 6 and 30 °C. It was found that the pseudo-second-order equation was better in describing the adsorption kinetics of reactive blue 19 on CC/OPA. The data obtained from adsorption isotherms at different temperatures were used to calculate thermodynamic quantities such as ΔG° , ΔH° and ΔS° of adsorption. The results indicate that RB19 adsorption onto CC/OPA is spontaneous and physical in nature.

Acknowledgement

The authors acknowledge the research grant provided by University Science Malaysia, under short-term grant that has resulted in this article.

References

- [1] P. Janos, H. Buchtova, M. Ryznarova, Sorption of dyes from aqueous solutions onto fly ash, *Water Res.* 37 (2003) 4938–4944.
- [2] H. Metivier-Pignon, C. Faur-Brasquet, P. Le Cloirec, Adsorption of dyes onto activated carbon cloths: approach of adsorption mechanisms and coupling of ACC with ultrafiltration to treat coloured wastewaters, *Sep. Purif. Technol.* 31 (2003) 3–11.
- [3] J. Orthman, H.Y. Zhu, G.Q. Lu, Use of anion clay hydrotalcite to remove coloured organics from aqueous solutions, *Sep. Purif. Technol.* 31 (2003) 53–59.
- [4] P. Waranusantigul, P. Pokethitiyook, M. Kruatrachue, E.S. Upatham, Kinetics of basic dye (methylene blue) biosorption by giant duckweed (*Spirodela polyrrhiza*), *Environ. Pollut.* 125 (2003) 385–392.
- [5] N. Koprivanac, A. Loncaric Bozic, S. Papic, Cleaner production processes in the synthesis of blue anthraquinone reactive dyes, *Dyes Pigments* 44 (2000) 33–40.
- [6] S. Netpradit, P. Thiravetyan, S. Towprayoon, Adsorption of three azo reactive by metal hydroxide sludge: effect of temperature, pH and electrolytes, *J. Colloid Interface Sci.* 270 (2004) 255–261.
- [7] S. Netpradit, P. Thiravetyan, S. Towprayoon, Application of ‘waste’ metal hydroxide sludge for adsorption of azo reactive dyes, *Water Res.* 37 (2003) 763–772.
- [8] T. Panswad, W. Luangdilok, Decolorization of reactive dyes with different molecular structures under different environmental conditions, *Water Res.* 34 (2000) 4177–4184.
- [9] Y.E. Benkli, M.F. Can, M. Turan, M.S. Celik, Modification of organo-zeolite surface for the removal of reactive azo dyes in fixed-bed reactors, *Water Res.* 39 (2005) 487–493.
- [10] V.K. Garg, M. Anita, R. Kumar, R. Gupta, Basic dye (methylene blue) removal from simulated wastewater by adsorption using Indian rosewood sawdust: a timber industry waste, *Dyes Pigments* 63 (2004) 243–250.
- [11] A.A. Ahmad, B.H. Hameed, N. Aziz, Adsorption of direct dye on palm ash: kinetic and equilibrium modeling, *J. Hazard. Mater.* 141 (2007) 70–76.
- [12] I. Uzun, F. Guzel, Kinetics and thermodynamics of the adsorption of some dyestuffs and *p*-nitrophenol by chitosan and MCM-chitosan from aqueous solution, *J. Colloid Interf. Sci.* 274 (2004) 398–412.
- [13] F.C. Wu, R.L. Tseng, R.S. Juang, Comparative adsorption of metal and dye on flake- and bead-types of chitosans prepared from fishery waste, *J. Hazard. Mater.* 73 (2000) 63–75.
- [14] X. Zeng, E. Ruckenstein, Cross-linked macroporous chitosan anion-exchange membranes for protein separations, *J. Membr. Sci.* 148 (1998) 195–205.

- [15] M.N.V. Ravi Kumar, A review of chitin and chitosan applications, *React. Funct. Polym.* 46 (2000) 1–27.
- [16] H. Yoshida, S. Fukuda, A. Okamoto, T. Kataoka, Recovery of direct dye and acid dye by adsorption on chitosan fiber-equilibria, *Water Sci. Technol.* 23 (1991) 1667–1676.
- [17] H. Yoshida, A. Okamoto, T. Kataoka, Adsorption of acid dye on cross-linked chitosan fibers: equilibria, *Chem. Eng. Sci.* 48 (1993) 2267–2272.
- [18] M.S. Chiou, H.Y. Li, Adsorption behavior of reactive dye in aqueous solution on chemical cross-linked chitosan beads, *Chemosphere* 50 (2003) 1095–1105.
- [19] M.Y. Chang, R.S. Juang, Adsorption of tannic acid, humic acid, and dyes from water using the composite of chitosan and activated clay, *J. Colloid Interf. Sci.* 278 (2004) 18–25.
- [20] M.S. Chiou, G.S. Chuang, Competitive adsorption of dye metanil yellow and RB15 in acid solutions on chemically cross-linked chitosan beads, *Chemosphere* 62 (2006) 731–740.
- [21] Z. Al-Qoda, Adsorption of dyes using shale oil ash, *Water Res.* 34 (2000) 4295–4303.
- [22] K.R. Hall, L.C. Eagleton, A. Acrivos, T. Vermeulen, Pore and solid diffusion kinetics in fixed-bed adsorption under constant pattern conditions, *Ind. Eng. Chem. Fundam.* 5 (1996) 212–223.
- [23] H.M.F. Freundlich, Über die adsorption in lösungen, *Z. Phys. Chem.* 57 (1906) 385–470.
- [24] M.I. Temkin, V. Pyzhev, Kinetics of ammonia synthesis on promoted iron catalyst, *Acta Physicochim.*, URSS 12 (1940) 327–356.
- [25] Y. Kim, C. Kim, I. Choi, S. Rengraj, J. Yi, Arsenic removal using mesoporous alumina prepared via a templating method, *Environ. Sci. Technol.* 38 (2004) 924–931.
- [26] O. Redlich, D.L. Peterson, A useful adsorption isotherm, *J. Phys. Chem.* 63 (1959) 1024.
- [27] S. Lagergren, Zur theorie der sogenannten adsorption gelöster stoffe, *K. Sven. Vetenskapsakad Handl.* 24 (1898) 1–39.
- [28] Y.S. Ho, Adsorption of heavy metals from waste streams by peat, PhD Thesis, University of Birmingham, Birmingham, UK, 1995.
- [29] G. McKay, Y.S. Ho, Pseudo-second order model for sorption processes, *Process Biochem.* 34 (1999) 451–465.
- [30] G. McKay, Y.S. Ho, The sorption of lead (II) on peat, *Water Res.* 33 (1999) 578–584.
- [31] S. Azizian, B. Yahyaee, Adsorption of 18-crown-6 from aqueous solution on granular activated carbon: a kinetic modeling study, *J. Colloid Interf. Sci.* 299 (2006) 112–115.
- [32] S. Azizian, Kinetic models of sorption: a theoretical analysis, *J. Colloid Interf. Sci.* 276 (2004) 47–52.
- [33] R. Niwas, U. Gupta, A.A. Khan, K.G. Varshney, The adsorption of phosphamidon on the surface of styrene supported zirconium tungstophosphate: a thermodynamic study, *Colloid Surf. A: Physicochem. Eng. Asp.* 164 (2000) 115–119.
- [34] M.J. Jaycock, G.D. Parfitt, *Chemistry of Interfaces*, Ellis Horwood, Chichester, 1981, pp. 12–13.
- [35] H. Nollet, M. Roels, P. Lutgen, P. Van der Meeren, W. Verstraete, Removal of PCBs from wastewater using fly ash, *Chemosphere* 53 (2003) 655–665.